

UCLA

UCLA Previously Published Works

Title

Implementation of two-dimensional L-COSY at 7 tesla: An investigation of reproducibility in human brain

Permalink

<https://escholarship.org/uc/item/0fh9h3gm>

Journal

Journal of Magnetic Resonance Imaging, 40(6)

ISSN

1053-1807

Authors

Verma, Gaurav
Hariharan, Hari
Nagarajan, Rajakumar
[et al.](#)

Publication Date

2014-12-01

DOI

10.1002/jmri.24510

Peer reviewed

Implementation of Two-Dimensional L-COSY at 7 Tesla: An Investigation of Reproducibility in Human Brain

Gaurav Verma, PhD,¹ Hari Hariharan, PhD,¹ Rajakumar Nagarajan, PhD,²
Ravi P.R. Nanga, PhD,¹ Edward J. Delikatny, PhD,¹ M. Albert Thomas, PhD,²
and Harish Poptani, PhD^{1*}

Purpose: To evaluate the utility of two-dimensional (2D) Localized Correlated Spectroscopy (L-COSY) in metabolic profiling of the human brain at 7 Tesla (T).

Materials and Methods: The 2D L-COSY sequence was implemented at 7T and its reliability was assessed by test–retest studies of a metabolite phantom and a healthy volunteer. L-COSY data were acquired from the occipital lobe of healthy subjects (n=6; all male; age, 30–72 years) to assess intersubject variability. Additionally, two subjects underwent scans from the parieto-occipital region, basal ganglia, frontal lobe or dorsolateral prefrontal cortex to test the versatility of L-COSY in studying differing anatomy. Integral/volume measurements of L-COSY spectra were used to estimate normalized metabolite-to-creatine concentrations.

Results: Phantom test–retest studies revealed coefficients of variation (CVs) of 3–20% for most metabolites. Human 2D L-COSY spectra permitted detection of several metabolite resonances from multiple locations and intersubject variation studies demonstrated CVs of 4–26%. Cross-peaks from gamma-aminobutyric acid (GABA), isoleucine (Ile), lysine (Lys) and Ethanolamine (Eth) were quantified, which are not readily resolvable with conventional one-dimensional (1D) MR spectroscopy.

Conclusion: 2D L-COSY at 7T demonstrated improved sensitivity in detecting additional metabolites with reliability comparable to established techniques at lower fields, which may aid in the metabolic assessment of diseased states.

Key Words: magnetic resonance spectroscopy; localized correlated spectroscopy; 7T; L-COSY; isoleucine; lysine
J. Magn. Reson. Imaging 2014;40:1319–1327.
© 2013 Wiley Periodicals, Inc.

THE ADVENT OF high field clinical MRI magnets, with field strengths of 7 Tesla (T) and above (1), promises linear increases in sensitivity and spectral resolution for in vivo MR spectroscopy (MRS). The improved sensitivity at 7T permits detection of low-concentration metabolites whose signal may be too weak to distinguish from background noise at lower fields, while increased chemical shift dispersion facilitates improved spectral separation of metabolites with similar chemical shifts on conventional one-dimensional (1D) MRS. Previous human brain 1D MRS studies at 7T with short echo time (TE) sequences have reported detection of a broad range of metabolites, including gamma-aminobutyric acid (GABA), glutamate (Glu), glutamine (Gln), glutathione (GSH), myo-inositol (mI), and phosphocholine (PC) (2–4). However, these peaks are subject to severe spectral overlap in 1D MRS due to their complex multiplet patterns and the presence of overlapping resonances.

In vivo two-dimensional (2D) MRS techniques (5,6), such as localized correlated spectroscopy (L-COSY), aid in further improving the metabolic characterization of the brain compared with 1D analogues (7,8). By adding a second spectral dimension through the indirect monitoring of t_1 evolution, 2D L-COSY detects the transfer of coherence between J -coupled metabolites. Coherence transfer manifests as “cross-peaks” in the 2D spectrum and helps facilitate the unambiguous assignment of metabolites whose primary resonances—“diagonal peaks” in the 2D spectrum—may otherwise appear co-resonant with other metabolites similar to that of 1D MRS. The 2D L-COSY sequence has been successfully implemented on the 1.5T and 3T MRI scanners to study the human brain (9–11). More recently, the 2D L-COSY sequence has also been implemented at 7T with specific applications described in soleus muscle (12).

¹Department of Radiology, University of Pennsylvania, Philadelphia, Pennsylvania, USA.

²Department of Radiological Sciences, University of California, Los Angeles, California, USA.

Contract grant sponsor: the Institute for Translational Medicine and Therapeutics (ITMAT) Transdisciplinary Program in Translational Medicine and Therapeutics; Contract grant number: UL1RR024134; Contract grant sponsor: T32 trainee grant; Contract grant number: MH019112.

*Address reprint requests to: H.P., Department of Radiology, B6 Blockley Hall, 423 Guardian Drive, Philadelphia, PA 19104. E-mail: poptanih@uphs.upenn.edu

Received July 29, 2013; Accepted October 9, 2013.

DOI 10.1002/jmri.24510

View this article online at wileyonlinelibrary.com.

The primary focus of this study was to implement 2D L-COSY on the 7T MRI scanner, and to assess its reliability in measuring cerebral metabolites in humans, particularly of those that are more difficult to characterize at lower field strengths.

MATERIALS AND METHODS

Pulse Sequence

Figure 1 shows the pulse sequence diagram for the 2D L-COSY sequence that was implemented on the 7T scanner. The 2D L-COSY sequence used a modified point resolved spectroscopic sequence (PRESS) (13) localization scheme consisting of 90° - 180° - 90° slice selective radiofrequency (RF) pulses, where the last pulse was changed from a refocusing 180° to a 90° pulse which facilitated the coherence transfer necessary for correlating the J -coupled metabolite peaks in the second dimension. The resulting coherence transfer echo was read out using the analog-to-digital converter (ADC). An incremental Δt_1 delay was introduced between the 180° and final 90° pulses to indirectly sample the t_1 dimension. Uncoupled spins do not experience any coherence transfer and consequently maintain equal intensity during t_1 evolution and read-out periods (t_2). These spins appear along the diagonal in the Fourier transformed spectrum. The coupled spins between which coherence transfer occurs during the t_1 evolution period exhibit different F_1 and F_2 frequencies and appear off the main diagonal as cross-peaks in the 2D spectrum after a double Fourier transformation. The Δt_1 increment used in the 7T studies was 0.4 ms resulting in a bandwidth of 2500 Hz along the indirect dimension (F_1).

Increased dielectric effects at higher fields result in increased B_1 field inhomogeneity (14), and thus the resulting inconsistent excitation profiles are a greater concern at 7T. The vendor-provided FASTESTMAP shimming method (Siemens Medical Solutions, Erlangen, Germany) was used to minimize spectral linewidths (15,16). To counteract shorter T_2 relaxation times at 7T (17–19), pulse lengths, gradient duration, and interpulse delays were reduced to a minimum, resulting in a TE of 18 ms, while maintaining desired gradient crusher durations and RF pulse shapes. The 180° RF pulse duration was 4.4 ms and associated crusher duration was 1.0 ms. The 90° coherence transfer pulse had a duration of 2.4 ms and crusher duration of 1.5 ms.

The bandwidth of the 180° RF pulse was restricted to 1200 Hz (4.0 ppm) and was centered at 2.35 ppm, which resulted in a more uniform excitation profile while preserving signal quality across most of the spectrum of interest. These bandwidth-limited pulses resulted in slightly reduced excitation of water at 4.7 ppm and the 0.0 ppm resonance of the 4,4-dimethyl-4-silapentane-1-sulfonic acid (DSS) used in the phantom studies. Because both the 90° RF and coherence transfer pulses had bandwidths of 2400 Hz (8.1 ppm), and the coherence transfer pulse in particular is responsible for generating the cross-peaks, the ratio between cross-peak and diagonal peak intensities is

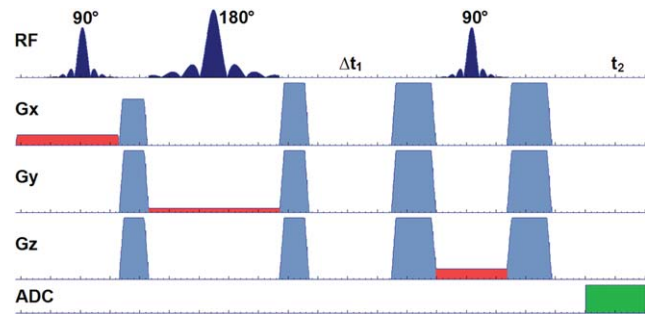


Figure 1. A pulse sequence diagram for the 2D L-COSY sequence showing the 90° - 180° - Δt_1 - 90° localization scheme. RF pulses and crusher gradients are shown in dark and light blue, respectively. Slice selective gradients along the three orthogonal directions are shown in red and the ADC is shown in green.

not affected by the bandwidth limitations. The refocusing pulse does not distort the cross-peak signals because coherence transfer is a nonlinear process in time and not reversible with a simple 180° RF. To further confirm the effect of lower bandwidth on measured metabolite ratios, a phantom study was conducted implementing RF pulse bandwidths ranging from 900 Hz to 2400 Hz, in intervals of 300 Hz. It was found that for signals near or inside the range of 0.65 ppm and 4.35 ppm, which includes all the metabolites quantified in this study, the metabolite to Cr ratio changed by less than 10% on average (data not shown).

Water suppression was performed using the variable pulse power and optimized relaxation delays (VAPOR) sequence (20), which implements seven RF pulses to reduce sensitivity to variations in the B_1 field. The scans were performed on Siemens 7T and 3T Tim-Trio whole-body MRI/MRS scanners (Siemens Medical Solutions, Erlangen, Germany) both operating on the VB17A platform. The 32-channel receive/volume transmit head coils were used to acquire all data for these studies.

Phantom Studies

Initial testing of the 2D L-COSY sequence was conducted using a “brain” phantom containing 16 metabolites at physiological concentrations (21–23). Table 1 lists these metabolites along with their chemical shifts and concentrations. The ΔF_1 and ΔF_2 values represent the range in frequency covered by the quantification region around the chemical shift of each peak. The bottom of Table 1 shows metabolites found in the human brain but which were not present in the phantom. Some metabolites appear multiple times in the table, indicating different cross-peaks that were each measured separately. For example, the cross-peak identified as “mI+Cho” represents the combined cross-peak of myo-Inositol (mI) and free choline (Cho) and this was measured separately from “mI” which is a cross-peak originating from myo-Inositol alone. Repeatability (test–retest) studies were performed by acquiring 30 L-COSY spectra from the phantom over 3 nonconsecutive days. Scan parameters for all

Table 1
Concentration (mM) and Diagonal (d) and Cross-Peaks (C) Chemical Shifts (ppm) of Metabolites in the Brain Phantom*

Metabolite name	Symbol	Pk	F2 (ppm)	F1 (ppm)	ΔF_2 (ppm)	ΔF_1 (ppm)	Conc. (mM)
4,4-dimethyl-4-silapentane-1-sulfonic acid	DSS	d	0.0	0.0	0.100	0.150	1.0
		C	1.8	0.6	0.100	0.150	1.0
		C	3.0	1.7	0.075	0.150	1.0
Lactate + threonine	Lac+Thr	d	1.3	1.3	0.075	0.200	0.4+0.9
		C	4.1	1.3	0.050	0.100	0.4+0.9
N-Acetylaspartate	NAA	d	2.0	2.0	0.075	0.200	7.6
		C	4.3	2.5	0.075	0.200	7.6
Glutamate	Glu	C	2.4	2.0	0.075	0.150	8.1
Glutamine	Gln	C	2.5	2.1	0.075	0.150	1.6
Gamma aminobutyric acid	GABA	C	3.0	1.9	0.050	0.100	0.7
Creatine	Cr	d	3.0	3.0	0.075	0.200	5.4
		C	3.9	3.9	0.050	0.200	5.4
Choline	Cho	d	3.2	3.2	0.075	0.200	0.9
Taurine	Tau	C	3.4	3.2	0.050	0.150	1.8
Myo-Inositol	ml	d	3.5	3.5	0.050	0.200	3.5
		C	3.6	3.2	0.075	0.150	3.5
Glutamate + glutamine	Glx	C	3.7	2.1	0.075	0.200	8.1+1.6
Aspartate	Asp	C	3.8	2.8	0.050	0.150	2.1
Ethanolamine	Eth	C	3.9	3.2	0.050	0.200	1.0
Phosphoethanolamine	PE	C	4.0	3.2	0.050	0.150	3.3
Myo-Inositol + free choline	ml+Cho	C	4.0	3.5	0.050	0.150	3.5+0.9
Phosphocholine	PC	C	4.3	3.6	0.050	0.100	3.3
Glutathione	GSH	C	4.5	2.9	0.100	0.250	2.0
Isoleucine	Ile	C	2.08	0.95	0.050	0.100	
Lysine	Lys	C	3.01	3.67	0.075	0.150	

*Additional metabolites detected only in human brain are listed at the bottom of the table.

phantom studies were identical and included: $2.0 \times 2.0 \times 2.0 \text{ cm}^3$ (8 mL) voxel size, 2000 ms repetition time (TR), 18 ms TE, 2048 t_2 points with 4000 Hz F_2 bandwidth, 64 Δt_1 increments with 2500 Hz F_1 bandwidth, 8 averages and a scan time of 17 min.

The same brain phantom was also scanned 27 times over three nonconsecutive days using a Siemens Tim-Trio 3T whole-body scanner, to facilitate a signal quality comparison between the two field strengths. F_2 and F_1 bandwidths were halved to 2000 Hz and 1250 Hz (Δt_1 increment=0.8 ms), respectively, to cover a similar range in ppm as the 7T study. Scan parameters, including timing (TE=18 ms, TR=2000 ms) and voxel size (8 mL), were otherwise kept identical to the 7T sequence and signal was acquired with a volumetric 32-channel head coil.

Human Volunteer Studies

All human studies were approved by the Institutional Review Board and this study was in compliance with the provisions of the Health Insurance Portability and Accountability Act (HIPAA). Written informed consent was obtained from all participants in the study.

One subject (age 31) was scanned seven times over 4 nonconsecutive days, and the L-COSY spectrum was acquired from the mid-occipital gray matter region to test the intrasubject reproducibility at 7T. A gradient-echo based localizer scan and a magnetization prepared rapid acquisition gradient echo (MPRAGE) sequence was acquired to facilitate the voxel placement. Each of these studies used $2.5 \times 2.5 \times 2.5 \text{ cm}^3$ (15.6 mL) voxels, repetition time (TR) of

2000 ms, echo time (TE) of 18 ms, 2048 t_2 points, 4000 Hz F_2 bandwidth, 64 Δt_1 increments, 2500 Hz F_1 bandwidth 8 averages and a 17 min scan time.

Six healthy volunteers (all male, age range 30 to 72 years, mean 40.5 ± 16.4) were recruited and each scanned once to test the intersubject variability of the 2D L-COSY sequence. Voxels of $3.0 \times 3.0 \times 3.0 \text{ cm}^3$ (27 mL) were localized in the mid-occipital gray matter region of each subject. Other scan parameters for these studies included: TR of 2000 ms, TE of 18 ms, 2048 t_2 points with 4000 Hz F_2 bandwidth, 64 Δt_1 increments with 2500 Hz F_1 bandwidth, 8 averages and a scan time of approximately 17 min.

As with the phantom study, the occipital lobe of one subject (age 46) was scanned using the same sequence on a 3T (Siemens Tim-Trio) scanner to compare in vivo signal quality between 3T and 7T. Scan parameters for the two field strengths were kept identical other than the reduction of F_2 , F_1 and water suppression bandwidths to accommodate the reduced spectral dispersion at 3T. The voxel size for the 3T study was $3.0 \times 3.0 \times 3.0 \text{ cm}^3$ (27 mL). No outer volume suppression (OVS) was applied in any of the studies and management of lipid contamination was performed through careful voxel placement alone.

Two subjects (ages 31 and 46) underwent additional 2D L-COSY studies at 7T from the basal ganglia, frontal lobe, dorsolateral prefrontal cortex (DLPFC) and parieto-occipital region to evaluate the versatility of the 2D L-COSY sequence in obtaining spectra from locations further away from the isocenter of the magnet (occipital lobe) and the imaging coil.

Postprocessing

The raw 2D L-COSY data extracted from the scanner was processed using a custom MATLAB-based post-processing program (Version 7.0, The Mathworks, Natick, MA). In the first step of postprocessing, the program extracted and combined real and imaginary time-domain signal from the raw data file. This signal was scaled by a constant value and the spectral oversampling and dummy points were removed. The signal was then averaged in the time domain.

Coil combination was performed using a custom method that preserved phase information along the t_1 dimension, in contrast to the zero-phasing scheme implemented by the Siemens image calculation environment (ICE). This method facilitated the use of multi-channel coils in acquiring the 2D data. Following coil combination, data were zero-filled and spectral line-broadening filters were applied before Fourier transformation along both t_2 and t_1 time dimensions (24,25). A sinebell filter was applied along the t_1 dimension and a skewed-squared sinebell filter (skew parameter = 0.3) along the t_2 dimension. The resulting two frequency dimensions (F_1 and F_2), were then plotted as magnitude-mode contour plots using MATLAB macros.

Using chemical shift information derived from the literature (21–23), diagonal and cross-peaks were assigned in the 2D spectra and quantified using a volume integral method (26), analogous to calculating peak areas in 1D MRS. Quantification regions were drawn around each identified peak and the total signal within these regions was calculated in magnitude mode. To avoid introducing measurement bias to the data, these regions were not moved from scan to scan, beyond an initial adjustment for center frequency using NAA as a reference at 2.0 ppm. Cross-peak integrals values were determined by averaging the signal of detectable cross-peaks above and below the diagonal. The reliability of the measurements was determined by calculating the coefficient of variation (CV) of the ratio between a given metabolite (standard deviation / mean) and the integral value of the Cr diagonal peak at 3.0 ppm (8). This value will hereafter be referred to as the CV of S/S_{Cr} .

RESULTS

The full width at half-maximum (FWHM) of the water signal in magnitude-mode 1D spectra for the phantom studies at 7T ranged between 5 and 7 Hz, while for the human studies it was 20–30 Hz. The water suppression scheme was generally very effective, with the residual peak of water showing a similar intensity as that of the NAA peak, indicating that over 99% of the water signal was suppressed. Water suppression resulted in the unavoidable partial suppression of the above diagonal cross-peaks of GSH at $[F_2, F_1] = (2.9 \text{ ppm}, 4.5 \text{ ppm})$ and NAA at $[F_2, F_1] = (2.5 \text{ ppm}, 4.3 \text{ ppm})$, because these resonances appear near the water peak at 4.7 ppm. Measurement of these metabolites therefore relied only on the quantification of the cross-peaks below the diagonal, which were clearly

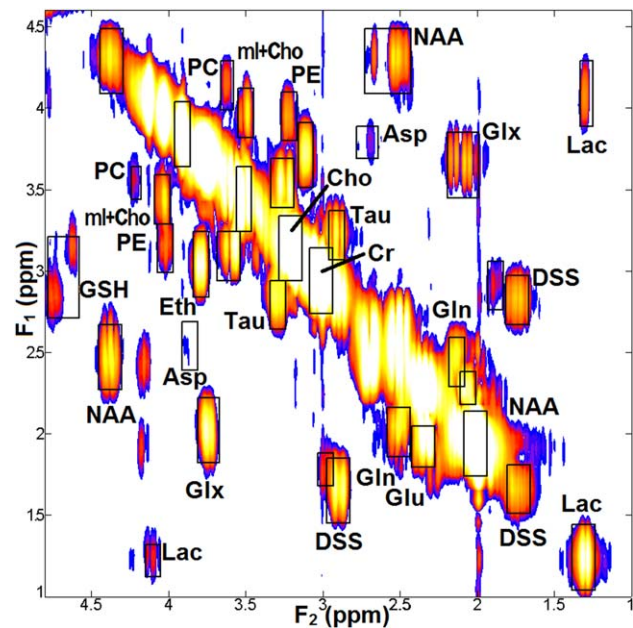


Figure 2. A representative 2D L-COSY spectrum from an 8.0-mL voxel in the brain phantom. Diagonal resonances of Cho, Cr, Lac+Thr, ml, and NAA are shown along with cross-peaks due to J -coupling in Asp, DSS, GABA, Glx (Glu+Gln), GSH, Eth, Lac+Thr, ml, ml+Cho, NAA, PC, PE, and Tau. Quantification regions for volume integral measurements are shown as black boxes around the metabolite peaks. [Color figure can be viewed in the online issue, which is available at wileyonlinelibrary.com.]

visible across all 7T studies because those peaks were unaffected by the water suppression.

Figure 2 shows a representative 2D L-COSY spectrum from the brain phantom. Diagonal and cross-peaks are labeled. For the peak quantification scheme, the range of chemical shifts was outlined using rectangular boxes for each identified metabolite peak, and the volume of the signal was quantified within the selected region. All of the metabolites present in the phantom (Table 1) were detected in each study, including the peaks due to choline-containing compounds (Cho, phosphocholine (PC), phosphoethanolamine (PE) and ethanolamine (Eth)). GSH at $[F_2, F_1] = (4.5 \text{ ppm}, 2.9 \text{ ppm})$ was identifiable from the well-suppressed water signal and resonances due to lactate (Lac) were clearly identifiable in the phantom, which contained no lipids. Cross-peaks due to Glu $[F_2, F_1] = (2.5 \text{ ppm}, 2.1 \text{ ppm})$ and Gln $[F_2, F_1] = (2.4 \text{ ppm}, 2.0 \text{ ppm})$ were observed with a spectral separation of approximately 0.1 ppm, allowing differentiation between them due to the low line-widths observed (6–8 Hz).

Figure 3 shows a 2D L-COSY spectrum obtained from the occipital lobe of a healthy volunteer. Several diagonal and cross-peak resonances were identified in the 2D spectra. All of the metabolite resonances quantified in the phantom were also visible in the occipital lobe, with the exception of DSS at $[F_2, F_1] = (3.1 \text{ ppm}, 1.8 \text{ ppm})$, an external standard, which is not expected in the healthy brain. The diagonal peak of Lac at $[F_2, F_1] = (1.3 \text{ ppm}, 1.3 \text{ ppm})$ was not consistently resolvable from the lipid signal in human brain and

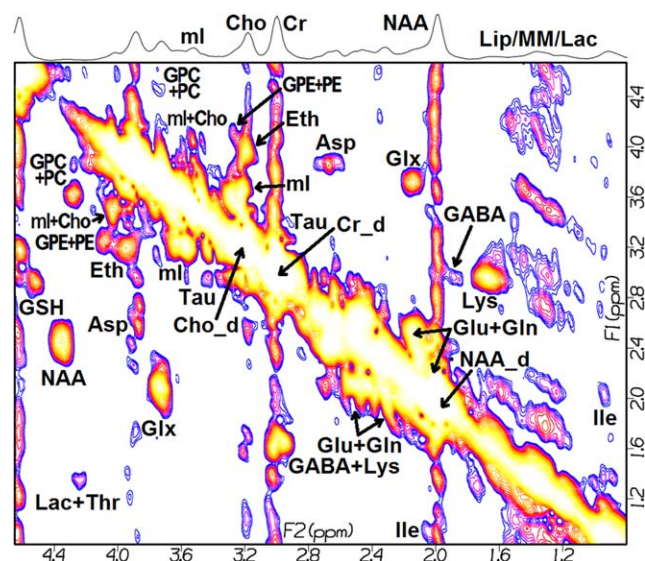


Figure 3. A 2D spectral plot acquired with L-COSY from the occipital lobe of a healthy volunteer (male; age, 32 years). Cross-peaks due to Ile and Lys are labeled in addition to the peaks also found in the brain phantom. A 1D projection of the 2D spectrum is shown at the top of the figure. [Color figure can be viewed in the online issue, which is available at wileyonlinelibrary.com.]

consequently not quantified in those studies, although the cross-peak of Lac at $[F_2, F_1] = (4.1 \text{ ppm}, 1.3 \text{ ppm})$ overlapping with that of Thr was quantified. The 2D cross-peaks due to the amino acids lysine (Lys) at $[F_2, F_1] = (3.0 \text{ ppm}, 1.7 \text{ ppm})$ and isoleucine (Ile) at $[F_2, F_1] = (2.04 \text{ ppm}, 0.95 \text{ ppm})$ were additionally detected in vivo from the human brain, which were not included in the brain phantom. Although GSH was detected in the L-COSY spectrum from all

the human subjects, adjacent t_1 -ridging associated with the residual water signal appeared more prominent and closer to GSH in humans than with the phantom. T_1 -ridging associated with the peaks of Cho, Cr, and NAA also appears as vertical lines at $F_2 = 3.2, 3.0,$ and 2.0 ppm , respectively.

Table 2 shows the CVs of S/S_{Cr} from phantom studies at 3T and 7T. CVs for the brain phantom ranged from 2.5 to 6.6% in diagonal peaks and 6.2 to 20.0% in cross-peaks at 7T. The highest CV observed was from GABA at 15.6%. By contrast, CVs from the 3T study ranged from 7.9 to 11.2% for diagonal peaks and 7.9 to 119.3% for cross-peaks. A direct comparison of signal to noise ratio (SNR) indicated that most metabolite peaks were 2–3 times more intense at 7T compared with 3T. At 3T, Asp, Lac, and PC had an SNR of 2.7 or less and CVs of 23.6% or more, suggesting low signal intensity contributed to their CV. GABA also had a relatively high CV at 24.3% while GSH had the highest CV at 119.3% at 3T. GSH was unique in having a higher measured SNR at 3T, suggesting the quantification region was contaminated by the inconsistent presence of residual water signal.

Table 3 shows the CVs of S/S_{Cr} in both intrasubject and inter subject human brain studies at 7T. CVs for the human intrasubject study from the occipital lobe ranged from 6.1 to 9.5% in diagonal peaks and 4.6 to 21.7% in cross-peaks. The inter-subject variation study resulted in CVs from 4.3 to 14.3% in diagonal peaks and from 6.6 to 26.3% for cross-peaks. GABA, GSH, Tau and the choline-containing metabolites produced among the highest CVs measured in both the intrasubject (5.7 to 19.2%) and inter-subject studies (24.0 to 26.3%). In the 2D human brain spectra, glycerophosphocholine (GPC) and glycerophosphoethanolamine (GPE) appeared co-resonant with the

Table 2
SNR of the Metabolites, Mean, SD, and CV of Metabolite to Creatine (3.0 ppm) Ratio From Metabolite Peaks Quantified From Brain Phantom Studies at 3T (N = 27) and 7T (N = 30)*

Name	Pk	3T brain phantom (N = 27)				7T brain phantom (N = 30)				7T/3T Gain
		SNR	/Cr 3.0	SD	CV	SNR	/Cr 3.0	SD	CV	
Lac	d	5.6	0.08	0.01	11.2	19.6	0.13	0.01	6.6	3.5
Lac	C	2.0	0.03	0.01	24.4	6.5	0.09	0.01	6.4	3.2
NAA	d	107.5	1.63	0.13	8.0	240.7	1.57	0.06	4.0	2.2
NAA	C	3.7	0.06	0.01	15.0	13.3	0.09	0.01	6.2	3.6
Glu	C	19.3	0.29	0.05	17.0	45.5	0.61	0.09	14.4	2.4
Gln	C	9.8	0.15	0.01	7.9	24.1	0.33	0.07	20.0	2.5
GABA	C	3.8	0.06	0.01	24.3	8.6	0.11	0.02	15.6	2.3
Cr 3.0	d	66.3	1.00	0.00	0.0	153.5	1.00	0.00	0.0	2.3
Cr 3.9	d	54.3	0.82	0.06	7.9	117.1	0.76	0.04	4.9	2.2
Cho	d	62.0	0.94	0.08	8.1	119.0	0.78	0.02	2.5	1.9
Tau	C	6.2	0.10	0.01	15.6	24.1	0.32	0.04	11.1	3.9
ml	d	25.0	0.38	0.04	9.7	79.4	0.52	0.02	3.0	3.2
ml	C	6.7	0.10	0.01	12.7	24.8	0.33	0.04	13.3	3.7
Glx	C	7.3	0.11	0.01	8.2	16.9	0.23	0.03	14.9	2.3
Asp	C	1.9	0.03	0.01	23.6	3.3	0.03	0.00	12.5	1.8
Eth	C	7.8	0.12	0.01	9.2	23.5	0.31	0.02	7.2	3.0
GPE/PE	C	4.3	0.07	0.01	13.2	16.2	0.21	0.01	6.9	3.7
ml+Cho	C	4.3	0.07	0.01	11.6	9.5	0.12	0.01	10.9	2.2
GPC/PC	C	2.7	0.04	0.01	26.6	5.9	0.08	0.01	12.0	2.2
GSH	C	7.7	0.12	0.14	119.3	3.7	0.02	0.00	12.1	0.5

*The 7T/3T column at right shows the ratio of SNR at 7T compared to 3T.

Table 3

Mean and SD of Metabolite Ratios Relative to the Creatine Diagonal Peak at 3.0 ppm and CVs (%) of S/S_{Cr} From Intrasubject and Intersubject Variability Studies (From the Occipital Lobe)*

Name	Pk	Intrasubject (N = 7)			Intersubject (N = 6)		
		Mean	SD	CV	Mean	SD	CV
Lac	C	0.02	0.00	11.3	0.01	0.00	16.0
NAA	d	1.45	0.13	8.9	1.37	0.20	14.3
NAA	C	0.05	0.00	4.6	0.05	0.01	12.1
Ile	C	0.05	0.01	15.0	0.05	0.01	21.2
Glu	C	0.29	0.04	13.1	0.23	0.04	18.2
Gln	C	0.23	0.01	3.9	0.20	0.02	9.3
Lys	C	0.11	0.02	13.5	0.10	0.01	6.6
GABA	C	0.10	0.02	21.6	0.07	0.01	16.6
Cho	d	0.69	0.05	7.5	0.64	0.03	4.3
Tau	C	0.10	0.02	21.7	0.09	0.02	22.9
ml	d	0.35	0.02	6.1	0.28	0.02	5.8
ml	C	0.24	0.02	9.3	0.24	0.06	24.8
Cr	d	0.89	0.08	9.5	0.79	0.09	11.1
Glx	C	0.21	0.01	5.6	0.17	0.02	10.5
Asp	C	0.05	0.00	8.5	0.05	0.01	22.7
Eth	C	0.08	0.01	16.6	0.08	0.02	26.3
GPE/PE	C	0.06	0.00	5.7	0.04	0.01	25.0
ml+Cho	C	0.06	0.01	13.4	0.05	0.01	24.0
GPC/PC	C	0.04	0.01	19.2	0.04	0.01	24.4
GSH	C	0.03	0.01	20.2	0.03	0.01	21.8

*Diagonal and cross-peaks are labeled as d and C, respectively. In the intersubject study, N refers to the number of subjects in the case of the intersubject study and the number of repeated scans of a single subject in the intrasubject study.

cross-peaks of PC and PE, respectively, so peak quantification combined the intensity of those pairs of metabolite peaks.

Figure 4 shows 2D spectra from the phantom as well as from the occipital lobe of the same subject at both 3T and 7T. The spectra were scaled such that the average noise in each spectrum would have identical intensity. The minimum contour threshold was selected to be just above the level at which background noise peaks would begin to appear in the spectra. Despite identical scan times and voxel sizes, spectra from the 7T scanner showed considerably better signal quality than their 3T counterparts. Consequently, cross-peaks due to Asp, GABA, GPC/PC, GPE/PE, Ile, Lac and ml+Cho, all of which were clearly identifiable in the 7T spectra were weak, obscured or absent from the 3T spectra.

Figure 5 shows a representative 2D spectrum acquired from the left basal ganglia of a healthy volunteer. The spectrum quality is similar to that observed in the reproducibility studies and demonstrates the same major diagonal and cross-peaks that were observed from the occipital lobe despite the smaller volume used. The quality of spectra from the parieto-occipital lobe, frontal lobe, and the dorsolateral prefrontal cortex (DLPFC, data not shown), also acquired with 15.6 mL voxels, were comparable to this spectrum.

DISCUSSION

In this study, we successfully demonstrated that the L-COSY sequence can reliably and reproducibly acquire 2D spectra from the brain at 7T. In addition, the sequence facilitated the unambiguous identifica-

tion and quantification of cross-peaks from several metabolites, including GABA, Glu, Gln, GSH, Ile, Lys, and choline containing compounds, with increased separation than has been reported with the same sequence at lower field strengths of 1.5T or 3T (8,27). The ability to noninvasively detect these additional metabolites presents several applications with potential clinical utility. For example, 1D MRS studies have reported elevated total choline in tumors (28) and ex vivo studies with high resolution NMR have shown variations within the choline-containing metabolites, like higher PC/GPC ratio, correlating with high-grade gliomas (28–30). High-resolution NMR has also been used to evaluate the concentration of Lys, Ile and other metabolites ex vivo in gliomas (29), and these findings may serve as a guideline for the noninvasive monitoring of the biochemical changes observed in brain tumors. Elevated GABA (31–33) and reduced GSH synthesis (34) and dysfunctional glutamatergic neurotransmission (35,36) have been implicated as markers for schizophrenia. Lys has been suggested as a biomarker for oxidative stress in nephropathy associated with Type II diabetes (37,38). The separation of Glu from Gln could have application in the field of neuropsychiatry as glutamatergic pathways have been suggested in the role of mood disorders (39,40) such as bipolar disorder and major depression.

The results of the present study can most closely be compared with 2D L-COSY reproducibility studies in the brain at 1.5T and 3T (8,27). Both the previous studies used a voxel size of 3.0 × 3.0 × 3.0 cm³ (27 mL) and 128 Δt₁ measurements for a total scan time of 34 min, with otherwise comparable scan parameters. At 1.5T, intersubject CVs ranged from 6–8% for diagonal peaks and 8–26% for cross-peaks while

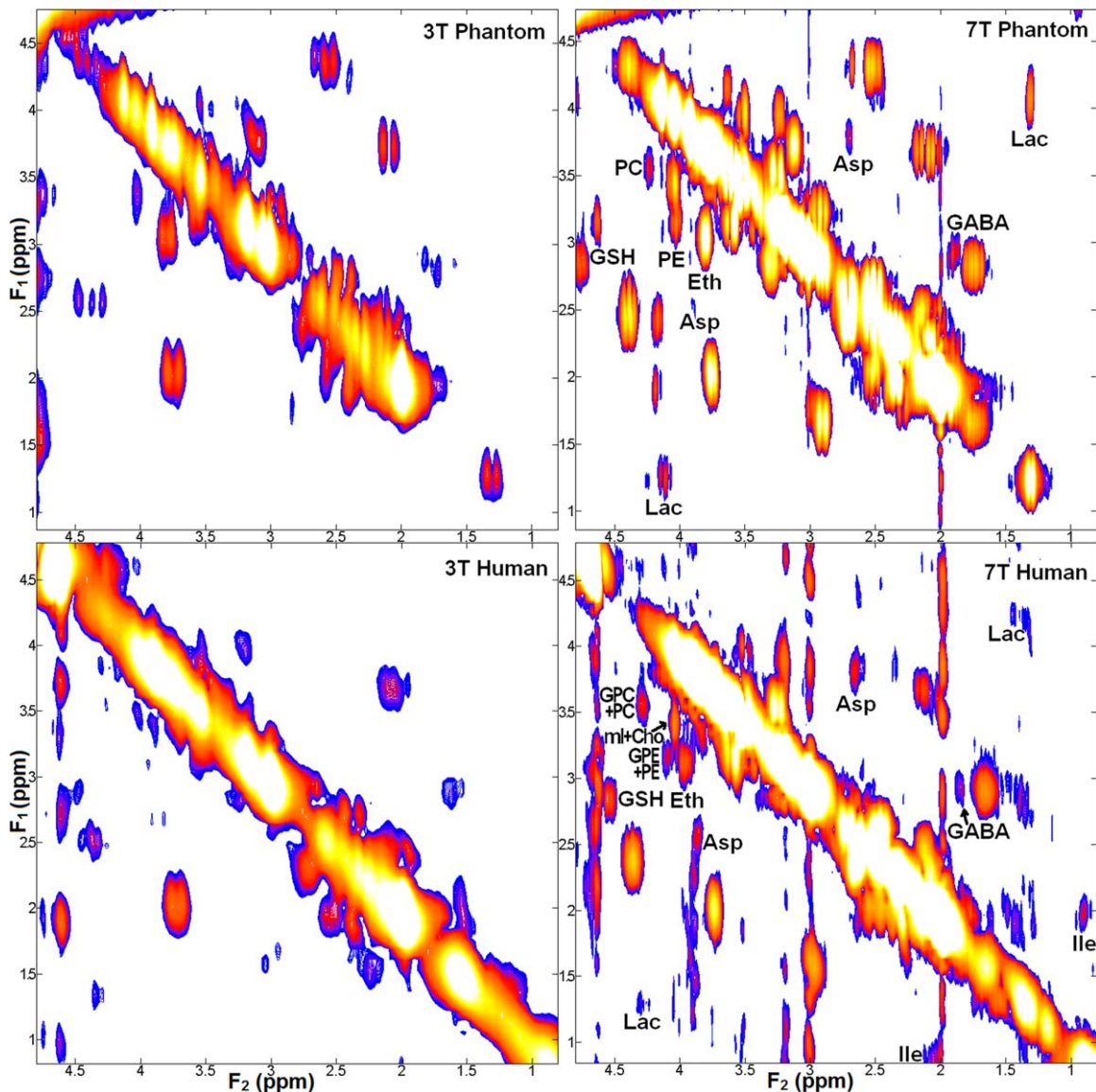


Figure 4. The 2D L-COSY spectra from 3T (left) and 7T (right) from a phantom (voxel size = 8 mL) (top) and human (voxel size = 27 mL) (bottom) study, normalized to the level of noise. Peaks readily identifiable at 7T but not at 3T are labeled. [Color figure can be viewed in the online issue, which is available at wileyonlinelibrary.com.]

intrasubject cross-peaks ranged from 3–4% for diagonal peaks and 4–27% for cross-peaks. At 3T, intersubject CVs ranged from 5–19% for diagonal peaks and 8–35% for cross-peaks. Our results with equal or smaller voxel size and half the scan time suggest improved sensitivity in detecting these metabolites at 7T. In addition, a direct comparison between 3T and 7T showed several metabolites readily quantifiable at 7T that were difficult to separate from nearby resonances due to lower spectral dispersion (like GABA, GSH, and Lys), difficult to resolve from background noise due to lower SNR (like Ile, Lac, Asp) or some combination of the two. Spectra from 7T did show increased t_1 ridging compared with their 3T counterparts. These are visible as vertical lines especially around the diagonal peak resonances of Cho, Cr, NAA, and water and are likely due to scanner fluctuations, such as unstable RF amplification, table vibration or subject movement (41).

It is worth noting that, similar to our results, the cross-peaks of the choline-containing metabolites (Cho, GPC/PC, GPE/PE and Eth) generated the highest CVs in the occipital lobe in both 1.5T (13–26%, (27)) and 3T (15% in occipital gray matter to 35% in occipital white matter, (8)) intersubject variation studies. The CVs for these metabolites in the phantom at 7T were considerably lower (7–13%), which may reflect a higher biological variation among these metabolites in humans as the age range of our human volunteers was from 30 to 72 years. CVs from intrasubject studies were generally lower than the corresponding CVs across different subjects at 1.5T and 7T (not measured in the 3T study), further suggesting the contribution of inherent variation to the intersubject CVs. Other metabolites with relatively higher CVs included GSH (not quantified at 1.5 T, 12–19% at 3T, 20–22% at 7T) and GABA (22–23% at 1.5T, not reported for 3T (8), 17–22% at 7T). The higher CV of

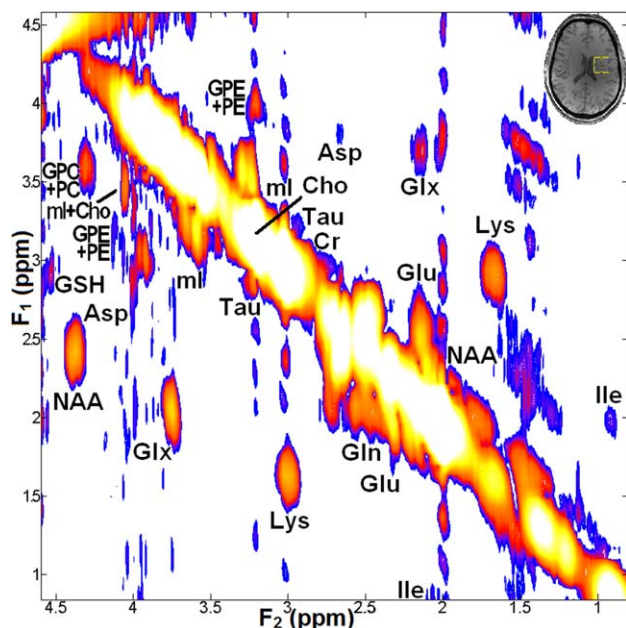


Figure 5. The 2D L-COSY spectrum from the basal ganglia region of a healthy volunteer (male, age 35 years), voxel size $2.5 \times 2.5 \times 2.5 \text{ cm}^3$ or 15.6 mL. [Color figure can be viewed in the online issue, which is available at wileyonlinelibrary.com.]

GABA may be attributable to its relatively low concentration (below 1 mM in healthy brain and in the phantom). These previous studies agree with the direct comparison of 3T and 7T performed with the brain phantom reproducibility study, and show that 7T L-COSY was able to reliably detect more metabolites than 1.5T and 3T with CVs of the additionally detected metabolites comparable to those metabolites detectable at lower field strengths. The proximity of the residual water signal to the GSH peak (~ 0.1 ppm separation) suggests that variability in the effectiveness of water suppression may be a significant factor in the measurement of GSH, though the measurement of GSH was more stable at 7T than at 3T in the phantom studies.

The FASTESTMAP technique was used to facilitate higher-order shim corrections, resulting in acceptable water line-widths even in diverse brain anatomy such as the basal ganglia and DLPFC. Careful shimming and maintaining small voxel size is critical to reliable signal acquisition from difficult-to-shim regions like the DLPFC and hippocampus which are of particular interest in schizophrenia (33). Multi-voxel-based MRSI sequences, using concentric circular echo-planar encoding or spiral encoding for faster acquisition, can facilitate smaller individual voxels by acquiring spectral data from a larger overall volume and higher spectral bandwidths at 7T (42,43).

Several limiting factors can contribute to the reliability of L-COSY at 7T. These include temporal instability due to field drift and imperfect shimming due to field inhomogeneity can affect line-widths and the effectiveness of water suppression. Human studies are subject to involuntary motion artifacts arising from the discomfort of a 17-min scan used in this study. Faster acquisition techniques, like average-

weighting and nonuniformly under-sampled acquisition and compressed sensing reconstruction (44) could mitigate these artifacts to some degree and improve the clinical viability of the sequence while reducing patient discomfort. Changes in temperature or pH could make precise placement of measurement volumes difficult and this is a limitation of rigid measurement volumes. Prior knowledge fitting (ProFit) (45), a 2D prior-knowledge based fitting algorithm, requires the development of basis sets containing all the metabolites detectable at 7T, but could prove useful in mitigating these potential sources of error. Reproducibility studies of the human brain at 7T using LC-Model (46), a commonly used algorithm for quantitative analysis of 1D MRS, analogous to ProFit, demonstrated CVs under 20% for most 1D-detectable metabolites (41,47). 1D MRS at 7T with conventional localization and spectral editing found CVs under 20% for NAA, Glu+Gln (Glx), Cr, Cho, ml, and GSH but not for other metabolites such as Asp, GABA, Lac, PE, and Tau, where CVs ranged from 29.4–93.8% for PRESS and 26.7–63.6% for TE-Averaging methods (41). The 1D MRS at 7T using very short echo times reported CVs ranging from 2.6 to 16.9% in the anterior cingulate and 3.4 to 44.1% in the dorsolateral prefrontal cortex (DLPFC). Neither of the 1D techniques at 7T reported detection or reliability measurements in Eth, Ile, or Lys (47).

In conclusion, this pilot study demonstrated the feasibility and reliability of 2D L-COSY in detecting additional metabolites in human brain than reported either by 1D studies at 7T or analogous 2D L-COSY studies at lower fields. Intersubject variation for quantified metabolite concentrations was in-line with variation of the same metabolites observed with this sequence at lower fields. Future development of the sequence will focus on improving scan performance, including both faster acquisition and smaller voxel size by implementing multi-voxel acquisition accelerated by concentric circular encoding based readouts. The 2D L-COSY sequence at 7T may aid in clinical applications including MRS studies in cancer and psychiatry where reliable detection and separation of individual choline containing compounds, separation of Lac from lipids, detection of Glu and GABA, could prove significant.

ACKNOWLEDGMENTS

This study was supported in part by a grant from the Institute for Translational Medicine and Therapeutics (ITMAT) Transdisciplinary Program in Translational Medicine and Therapeutics. G.V. was supported from a T32 trainee grant. Jenny Li, UCLA is acknowledged for her assistance in metabolite quantification. Tejiun Zhao of Siemens is acknowledged for providing the FASTESTMAP shim WIP package.

REFERENCES

1. Deelchand DK, Moortele PFV, Adriany G, et al. In vivo $(1)\text{H}$ NMR spectroscopy of the human brain at 9.4 T: Initial results. *J Magn Reson* 2010;206:74–80.

2. Mekle R, Mlynarik V, Gambarota G, Hergt M, Krueger G, Gruetter R. MR spectroscopy of the human brain with enhanced signal intensity at ultrashort echo times on a clinical platform at 3T and 7T. *Magn Reson Med* 2009;61:1279–1285.
3. Boer VO, Siero JCW, Hoogduin H, van Gorp JS, Luijten PR, Klomp DWJ. High-field MRS of the human brain at short TE and TR. *NMR Biomed* 2011;24:1081–1088.
4. Tkac I, Oz G, Adriany G, Ugurbil K, Gruetter R. In vivo ¹H NMR spectroscopy of the human brain at high magnetic fields: metabolite quantification at 4T vs. 7T. *Magn Reson Med* 2009;62:868–879.
5. Ernst RR, Bodenhausen G, Wokaun A. Principles of nuclear magnetic resonance in one and two dimensions. Oxford: Clarendon Press; 1987. 640 p.
6. Friebolin H, Beconsall JK. Basic one-and two-dimensional NMR spectroscopy. New York: Wiley Online Library; 1993. 442 p.
7. Thomas MA, Yue K, Binesh N, et al. Localized two-dimensional shift correlated MR spectroscopy of human brain. *Magn Reson Med* 2001;46:58–67.
8. Thomas M, Hattori N, Umeda M, Sawada T, Naruse S. Evaluation of two-dimensional L-COSY and JPRESS using a 3 T MRI scanner: from phantoms to human brain in vivo. *NMR Biomed* 2003;16:245–251.
9. Thomas MA, Chung HK, Middlekauff H. Localized two-dimensional ¹H magnetic resonance exchange spectroscopy: a preliminary evaluation in human muscle. *Magn Reson Med* 2005;53:495–502.
10. Thomas MA, Lange T, Velan SS, et al. Two-dimensional MR spectroscopy of healthy and cancerous prostates in vivo. *Magn Reson Mater Phys Biol Med* 2008;21:443–458.
11. Velan SS, Durst C, Lemieux SK, et al. Investigation of muscle lipid metabolism by localized one-and two-dimensional MRS techniques using a clinical 3T MRI/MRS scanner. *J Magn Reson Imaging* 2006;25:192–199.
12. Ramadan S, Ratai EM, Wald LL, Mountford CE. In vivo 1D and 2D correlation MR spectroscopy of the soleus muscle at 7T. *J Magn Reson* 2010;204:91–98.
13. Bottomley PA. Spatial localization in NMR spectroscopy in vivo. *Ann N Y Acad Sci* 1987;508:333–348.
14. Vaughan JT, Garwood M, Collins C, et al. 7T vs. 4T: RF power, homogeneity, and signal-to-noise comparison in head images. *Magn Reson Med* 2001;46:24–30.
15. Gruetter R. Automatic, localized in vivo adjustment of all first- and second-order shim coils. *Magn Reson Med* 2005;29:804–811.
16. Gruetter R, Tkac I. Field mapping without reference scan using asymmetric echo-planar techniques. *Magn Reson Med* 2000;43:319–323.
17. Rutgers D, Van der Grond J. Relaxation times of choline, creatine and N-acetyl aspartate in human cerebral white matter at 1.5 T. *NMR Biomed* 2002;15:215–221.
18. Mlynarik V, Gruber S, Moser E. Proton T1 and T2 relaxation times of human brain metabolites at 3 Tesla. *NMR Biomed* 2001;14:325–331.
19. Michaeli S, Garwood M, Zhu XH, et al. Proton T2 relaxation study of water, N-acetylaspartate, and creatine in human brain using Hahn and Carr-Purcell spin echoes at 4T and 7T. *Magn Reson Med* 2002;47:629–633.
20. Tkac I, Starcuk Z, Choi I, Gruetter R. In Vivo (¹H) NMR spectroscopy of rat brain at 1 ms echo time. *Magn Reson Med* 1999;41:649–656.
21. Govindaraju V, Young K, Maudsley AA. Proton NMR chemical shifts and coupling constants for brain metabolites. *NMR Biomed* 2000;13:129–153.
22. Velan SS, Lemieux SK, Raylman RR, et al. Detection of cerebral metabolites by single-voxel-based PRESS and COSY techniques at 3T. *J Magn Reson Imaging* 2007;26:405–409.
23. Remy C, Grand S, Lai ES, et al. ¹H MRS of human brain abscesses in vivo and in vitro. *Magn Reson Med* 2005;34:508–514.
24. Delikatny E, Hull W, Mountford CE. The effect of altering time domains and window functions in two-dimensional proton COSY spectra of biological specimens. *J Magn Reson* 1991;94:563–573.
25. Delikatny EJ, Watzl JQ. Application of 2D magnetic resonance spectroscopy to the study of human biopsies. *Mod Magn Reson* 2006;1015–1025.
26. Boyd J, Redfield C. Analysis of cross peak fine structure in multiple-quantum filtered COSY spectra. *J Magn Reson* 1986;68:67–84.
27. Binesh N, Yue K, Fairbanks L, Thomas MA. Reproducibility of localized 2D correlated MR spectroscopy. *Magn Reson Med* 2002;48:942–948.
28. Poptani H, Gupta RK, Roy R, Pandey R, Jain VK, Chhabra DK. Characterization of intracranial mass lesions with in vivo proton MR spectroscopy. *AJNR Am J Neuroradiol* 1995;16:1593–1603.
29. Martínez-Bisbal MC, Martí-Bonmatí L, Piquer J, et al. ¹H and ¹³C HR-MAS spectroscopy of intact biopsy samples ex vivo and in vivo ¹H MRS study of human high grade gliomas. *NMR Biomed* 2004;17:191–205.
30. Righi V, Roda JM, Paz J, et al. ¹H HR-MAS and genomic analysis of human tumor biopsies discriminate between high and low grade astrocytomas. *NMR Biomed* 2009;22:629–637.
31. Ongür D, Prescott AP, McCarthy J, Cohen BM, Renshaw PF. Elevated gamma-aminobutyric acid levels in chronic schizophrenia. *Biol Psychiatry* 2010;68:667–670.
32. Simpson M, Slater P, Deakin J, Royston M, Skan W. Reduced GABA uptake sites in the temporal lobe in schizophrenia. *Neurosci Lett* 1989;107:211–215.
33. Reynolds GP, Czudek C, Andrews HB. Deficit and hemispheric asymmetry of GABA uptake sites in the hippocampus in schizophrenia. *Biol Psychiatry* 1990;27:1038–1044.
34. Gysin R, Kraftsik R, Sandell J, et al. Impaired glutathione synthesis in schizophrenia: convergent genetic and functional evidence. *Proc Natl Acad Sci U S A* 2007;104:16621–16626.
35. Goff DC, Coyle JT. The emerging role of glutamate in the pathophysiology and treatment of schizophrenia. *Am J Psychiatry* 2001;158:1367–1377.
36. Kim J, Kornhuber H, Schmid-Burgk W, Holzmüller B. Low cerebrospinal fluid glutamate in schizophrenic patients and a new hypothesis on schizophrenia. *Neurosci Lett* 1980;20:379–382.
37. Wautier M, Massin P, Guillausseau P, et al. N (carboxymethyl) lysine as a biomarker for microvascular complications in type 2 diabetic patients. *Diabetes Metab* 2003;29:44–52.
38. Shaw JN, Baynes JW, Thorpe SR. N epsilon-(carboxymethyl) lysine (CML) as a biomarker of oxidative stress in long-lived tissue proteins. *Methods Mol Biol* 2002;186:129–137.
39. Auer DP, Pütz B, Kraft E, Lipinski B, Schill J, Holsboer F. Reduced glutamate in the anterior cingulate cortex in depression: an in vivo proton magnetic resonance spectroscopy study. *Biol Psychiatry* 2000;47:305–313.
40. Yuksel C, Ongur D. Magnetic resonance spectroscopy studies of glutamate-related abnormalities in mood disorders. *Biol Psychiatry* 2010;68:785–794.
41. Mehlkopf A, Korbee D, Tiggelman T, Freeman R. Sources of t1 noise in two-dimensional NMR. *J Magn Reson* 1984;58:315–323.
42. Xu D, Vigneron DB. High field MR spectroscopy: investigating human metabolite levels at high spectral and spatial resolution. *High-Field MR Imaging* 2012:215–228.
43. Furuyama JK, Wilson NE, Thomas MA. Spectroscopic imaging using concentric circular echo-planar trajectories in vivo. *Magn Reson Med* 2012;67:1515–1522.
44. Kazimierzczuk K, Orekhov VY. Accelerated NMR spectroscopy by using compressed sensing. *Angew Chem Int Ed Engl* 2011;50:5556–5559.
45. Schulte RF, Boesiger P. ProFit: two-dimensional prior-knowledge fitting of J-resolved spectra. *NMR Biomed* 2006;19:255–263.
46. Provencher SW. A constrained regularization method for inverting data represented by linear algebraic or integral equations. *Comput Phys Commun* 1982;27:213–227.
47. Wijtenburg SA, Rowland LM, Edden RAE, Barker PB. Reproducibility of brain spectroscopy at 7T using conventional localization and spectral editing techniques. *J Magn Reson Imaging* 2013;38:460–467.